CHEMISTRY OF MATERIALS

Article

pubs.acs.org/cm

Mechanically Tough and Chemically Stable Anion Exchange Membranes from Rigid-Flexible Semi-Interpenetrating Networks

Jing Pan,[†,‡] Liang Zhu,[†] Juanjuan Han,[‡] and Michael A. Hickner*[,†]

[†]Department of Materials Science and Engineering, The Pennsylvania State University, University Park, Pennsylvania 16802, United States

[‡]College of Chemistry and Molecular Sciences, Hubei Key Lab of Electrochemical Power Sources, Wuhan University, Wuhan 430072, China

Supporting Information

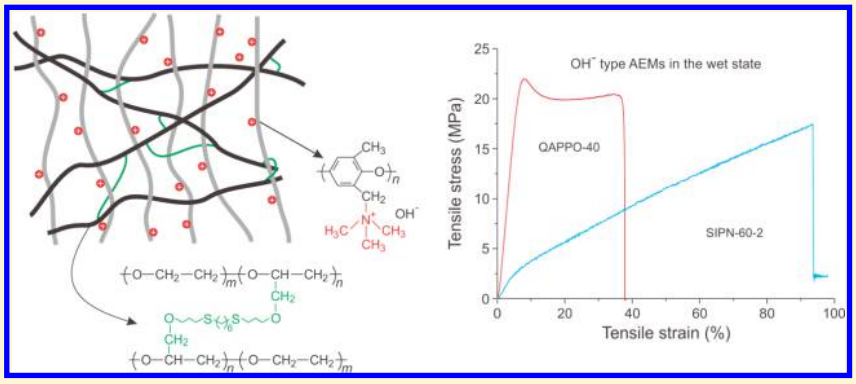

ABSTRACT: A series of tough and chemically stable semi-interpenetrating network anion exchange membranes (SIPN AEMs) composed of a rigid and ion-conductive component, quaternized poly(2,6-dimethyl phenylene oxide) (QAPPO), and a hydrophilic, cross-linked, flexible poly(ethylene glycol)-*co*-poly(allyl glycidyl ether) (*x*PEG−PAGE) component were synthesized. The SIPN AEMs containing both rigid and flexible polymer constituents exhibited outstanding mechanical strength and flexibility and were much tougher than conventional QAPPO membranes. The introduction of the hydrophilic network ensured SIPN AEMs with high hydration numbers, which contributed to the high ion conductivity of these materials. The physical properties of the SIPN AEMs could be varied by the mass fractions of the QAPPO and *x*PEG−PAGE components, and a trade-off was observed between the samples' conductive and swelling properties. Among the compositions studied, SIPN-60-2 ($Mass_{QAPPO\text{-}60}/Mass_{PEG-PAGE}$ = 2:1) with an IEC of 1.43 mmol/g was found to have balanced ionic conductivity (67.7 mS/cm at 80 °C) and swelling ratio (26% at 80 °C). The alkaline stabilities of the SIPN AEMs were evaluated in 1 M NaOH at 80 °C for 30 days. Good mechanical (72% and 74% retention in tensile strength and elongation at break, respectively) and dimensional (11% increase in water uptake) stability was retained by the SIPN AEM due to the presence of the alkali-resistant *x*PEG−PAGE network. The quaternary ammonium groups in SIPN-60-2 were found to be relatively stable (24% and 26% decrease in IEC and OH^- conductivity in 1 M NaOH at 80 °C for 30 days, respectively), and the low initial IEC and the high dimensional stability of the membrane protected the cation from severe degradation during the extended aging test.

INTRODUCTION

Fuel cells are a class of clean and highly efficient energy conversion devices that directly convert chemical energy stored in fuels into electricity. Proton exchange membrane fuel cells (PEMFCs) have many advantages, such as their high power and energy densities and the capability of room-temperature startup and low-temperature operation, which are considered to be ideal traits for vehicles and portable devices.[1−3] The most popular types of proton exchange membranes (PEM) employed in PEMFCs are Nafion, a perfluorinated sulfonic acid (PFSA)-based membrane, and other PFSA variants. Nafion exhibits excellent properties, such as high proton conductivity (~0.1 S/cm at operation temperature), moderate water uptake (38 mass % water uptake and ~15% swelling ratio), high strength (~25 MPa tensile strength) and flexibility (~180% elongation at break), and good chemical stability, which guarantees high PEMFC operational performance and long-term durability.[4−6] However, the strong acidic environment of a PEMFC allows only some noble metals, in particular platinum (Pt), as both stable and highly efficient catalysts for the electrode reactions. The scarcity and the high cost of exotic catalysts and the potential environmental impacts of perfluorinated polymers become major obstacles preventing the widespread application of PEMFCs.[7−9] Non-Pt group metal

Received: July 6, 2015
Revised: September 16, 2015
Published: September 17, 2015

DOI: 10.1021/acs.chemmater.5b02557
Chem. Mater. 2015, 27, 6689−6698

catalysts that are efficient and stable in acidic environments[10,11] and chemically stable aromatic proton-conducting membranes[12−14] are solutions to lower the current high costs of noble metal catalysts and perfluorinated membranes in PEMFCs, but these efforts remain in the domain of research for future PEMFC systems.

Anion exchange membrane fuel cells (AEMFCs) facilitate a high pH environment that allows for stable operation of catalysts composed of nonprecious metal or their oxides. The major advantage of AEMFCs is that they can lower the cost of fuel cell technologies by circumventing the Pt-dependent problem faced by the PEMFC system.[15−19] In the past decade, great efforts have been devoted to the realization of practical AEMFC technology; among them, the development of high-performance anion exchange membranes (AEMs) have drawn a lot of attention.[20−22] Usually, AEMs contain rigid backbone polymers, such as polysulfone,[23−25] poly(phenylene oxide),[26−29] polystyrene,[30−32] poly(ether ketone),[33−35] or poly(phenylene),[36] and employ cationic groups, such as quaternary ammonium (QA),[37,38] imidazolium,[39−41] phosphonium,[25,28] or guandinium[42,43] as the organic base. Compared to their acidic counterpart PEMs, AEMs generally show inferior properties. First, the lower mobility of OH^- and the less-developed morphology of aromatic polymers compared to perfluorinated structures naturally lead to lower ionic conductivity in AEMs. To increase conductivity of AEMs while preserving an acceptable swelling ratio, researchers have been attempting to fabricate AEMs with various cross-linked[44,45] and/or controlled microphase separated morphologies.[27,46,47] Second, the rigid polymer backbones ensure good mechanical strength (higher than 20 MPa), but the flexibility (lower than 30% elongation at break) of the AEMs is usually unsatisfactory.[27,48−53] Poor flexibility makes AEMs brittle, especially under low relative humidity conditions, which causes problems during MEA fabrication and long-term fuel cell operation under conditions such as wet−dry cycling. A possible and straightforward solution to this brittleness problem is to introduce membrane supports or flexible structures into rigid AEMs. For example, polytetrafluoroethylene (PTFE) porous film has been employed as a support material to produce composite AEMs.[54,55] Albeit having better mechanical properties, PTFE composite AEMs are known to suffer from poor compatibility between the fluorocarbon support and the aromatic backbone. Moreover, the PTFE framework presents a tortuous path for OH^- conduction through the ionic polymer phase, which could result in the decline of membrane conductivity. Finally, in addition to mechanical properties, the chemical stability of the cation and polymer backbone of AEMs under fuel cell operation conditions is a fast-growing topic.[56,57] From an engineering point of view, the chemical stability of the membrane could be at least as important as conductivity, if not more important to promote the longevity of the device.

Here, we report a unique approach to toughen AEMs by increasing their elongation to break while also boosting their chemical stability. A novel rigid-flexible semi-interpenetrating network (SIPN) was designed with a rigid, conductive functional segment, i.e., quaternary ammonium poly(phenylene oxide) (QAPPO), and a hydrophilic, flexible network, i.e., cross-linked poly(ethylene glycol)-*co*-poly(allyl glycidyl ether) (*x*PEG−PAGE). The SIPN AEM exhibited outstanding mechanical and conductive metrics and excellent chemical, and mechanical stabilities have been verified by testing the SIPN AEM samples under elevated temperature (80 °C) in alkaline solutions.

EXPERIMENTAL SECTION

Materials. Poly(2,6-dimethyl phenylene oxide) (PPO, powder) was purchased from Sigma-Aldrich (St. Louis, MO) and dried under a vacuum at room temperature overnight. Allyl glycidyl ether (AGE) was purchased from Sigma-Aldrich, degassed through several freeze−pump−thaw cycles, and distilled from butyl magnesium chloride (2.0 mol/g in THF, Sigma-Aldrich) before use. Poly(ethylene glycol) (PEG, M_w = 4000 g/mol), N-bromosuccinimide (NBS), 2,2′-azobis(2-methylpropionitrile) (AIBN), sodium hydride (60% dispersion in mineral oil), 1,6-hexanedithiol, and trimethylamine (TMA, 33% w/w in ethanol) were purchased from Sigma-Aldrich and used as received. The solvents and other chemicals used in this work were obtained from VWR International (Radnor, PA) and used as received.

Synthesis of Quaternized PPO (QAPPO). Brominated PPO (BrPPO) samples with different degrees of bromination (DB) ranging from 30 to 95% were prepared following the literature.[58] To synthesize quaternized PPO, BrPPO with the desired DB was dissolved in NMP to form a 5 wt % solution, into which TMA was added and stirred for 4 h at 45 °C to produce QAPPO solution. The QAPPO solutions produced with the BrPPO with DBs of 30, 40, 60, and 95% were cast onto a clean, flat glass plate and dried in a convection oven at 80 °C for 24 h and then further dried in a vacuum oven at 80 °C overnight to form the QAPPO-30, QAPPO-40, QAPPO-60, and QAPPO-95 AEMs, respectively. To replace the Br^- anion with OH^-, each membrane was immersed in 1 M NaOH solution at room temperature for 10 h. This process was repeated four times to ensure a complete displacement of the anion. Finally, the AEMs with the OH^- anion were repeatedly rinsed with deionized water until the pH of the residual water was neutral.

Synthesis of Poly(ethylene glycol)-*co*-poly(allyl glycidyl ether) (PEG−PAGE).[59] A total of 4 g of PEG precursor kept in the melt state at a temperature of 100 °C was degassed with Ar for 1 h. A total of 0.04 g of NaH was then transferred quickly to the PEG melt and reacted with PEG for 1 h. Subsequently, 30 mL of AGE was added to initiate the polymerization, and the polymerization reaction was conducted for 48 h. The copolymer was then precipitated in hexane from methanol to remove the unreacted AGE monomer and dried in a vacuum at 60 °C for 48 h. The molecular weight of the resulted PEG−PAGE was measured by ^{1}H NMR and gel permeation chromatography (GPC).

Synthesis of Semi-interpenetrating Network (SIPN)-based AEMs. PEG−PAGE was first dissolved in NMP to form a 10 wt % solution, and QAPPO solution (5 wt %) was then added. The solution was stirred at 40 °C for 2.5 h to give a solution blend of QAPPO and PEG−PAGE (QAPPO and PEG−PAGE). After adding 1,6-hexanedithiol into the blend solution, the mixture was stirred for 2 h and then cast onto a clean, flat glass plate and dried in a convection oven at 80 °C for 24 h and further dried in a vacuum oven at 80 °C overnight. The SIPN-based AEMs fabricated by QAPPO-60 are denoted as SIPN-60-1 ($W_{QAPPO\text{-}60}/W_{PEG-PAGE}$ = 1:1), SIPN-60-2 ($W_{QAPPO\text{-}60}/W_{PEG-PAGE}$ = 2:1), and SIPN-60-3 ($W_{QAPPO\text{-}60}/W_{PEG-PAGE}$ = 3:1), while those made by QAPPO-95 are denoted as SIPN-95-1 ($W_{QAPPO\text{-}95}/W_{PEG-PAGE}$ = 1:1) and SIPN-95-2 ($W_{QAPPO\text{-}95}/W_{PEG-PAGE}$ = 2:1). To replace the Br^- anion with OH^-, the membrane was immersed in a 1 M NaOH solution for 10 h. This process was repeated four times to ensure a complete displacement of the Br^- with OH^-. Finally, the AEMs in the OH^- anion form were repeatedly rinsed with deionized water until the pH of residual water was neutral.

Synthesis of cross-linked PEG−PAGE (*x*PEG−PAGE). PEG−PAGE was dissolved in NMP to form a 10 wt % solution. After adding 1,6-hexanedithiol into the solution, the mixture was stirred for 2 h. The resulting solution was then cast onto a clean, flat glass plate and dried in a convection oven at 80 °C for 24 h and further dried in a vacuum oven at 80 °C overnight to form the *x*PEG−PAGE membrane.

Characterization and Measurements. ^{1}H NMR spectra were measured at 300 MHz on a Bruker AV 300 spectrometer using

DOI: 10.1021/acs.chemmater.5b02557
Chem. Mater. 2015, 27, 6689−6698

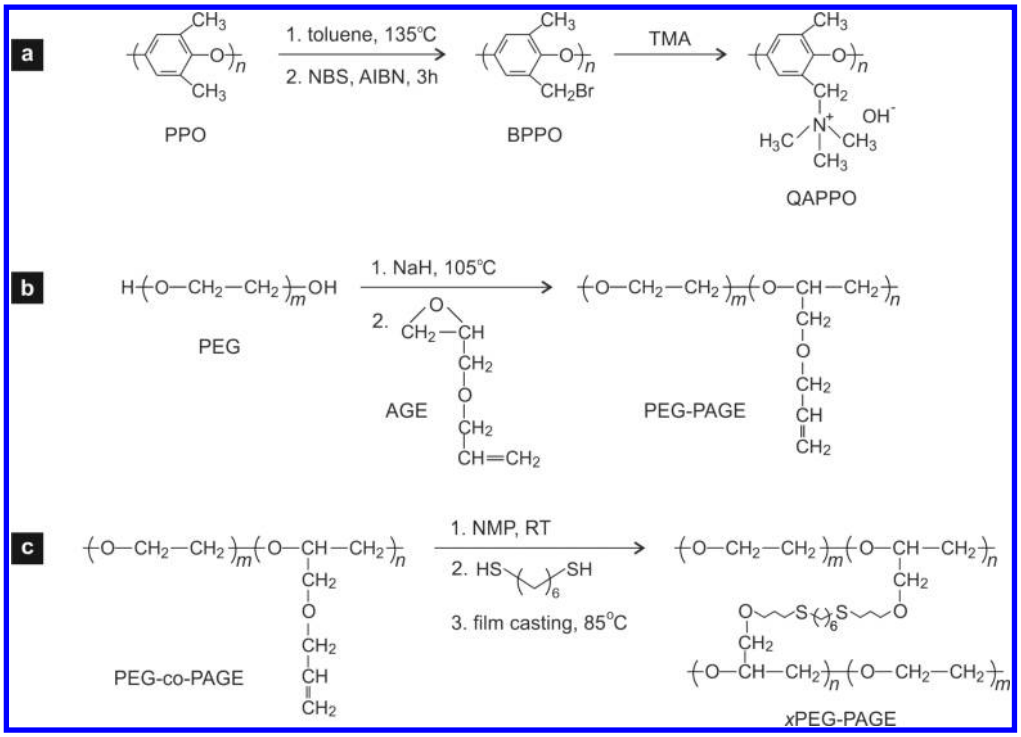

Figure 1. Preparation of (a) rigid quaternized poly(2,6-dimethyl phenylene oxide) (QAPPO), (b) flexible poly(ethylene glycol)-*co*-poly(allyl glycidyl ether) (PEG−PAGE), and (c) cross-linked PEG−PAGE (*x*PEG−PAGE).

DMSO-d_6 or $CDCl_3$ as the solvent. Fourier transform infrared (FT-IR) spectra were obtained on a Nicolet 6700 FTIR spectrometer with a wavenumber resolution of 4 cm^{-1} and spectral range of 400−4000 cm^{-1}. X-ray photoelectron spectroscopy (XPS) measurements were carried out using a Kratos XSAM-800 spectrometer with an Mg−Kα radiator. The S(2p) signal was collected and analyzed using XPS Peak software. GPC measurements were conducted on a Waters (Milford, MA) GPC system with a refractive index (RI) detector to determine the molecular weight and polydispersity indices of the brominated samples. The measurements were calibrated with poly(styrene) standards (Varian, Lake Forest, CA) in tetrahydrofuran (THF) solvent with a flow rate of 1 mL/min at 35 °C. The morphologies of the surface and cross sections of the AEMs were studied by scanning electron microscopy (SEM, FEI, Quanta 200). For transmission electron microscopy (TEM) observations, an AEM solution was cast to form a thin film on a Cu grid, followed by exchanging the anions with I^- by immersing the AEM-coated Cu grid in 1 M NaI solution. The samples were then subjected to TEM observations. Images were recorded using a JEOL JEM-2010FEF transmission electron microscope with an accelerating voltage of 200 kV. Small-angle X-ray scattering curves of unstained dry chloride-form membranes were obtained using a Rigaku (formerly Molecular Metrology) instrument equipped with a pinhole camera with an Osmic microfocus Cu K_α source and a parallel beam optic. Typical counting times for integration over a multiwire area detector were 1 h with typical membrane thicknesses on the order of 100 μm. Measurements were taken under vacuum conditions at ambient temperature on dry samples. Scattering intensities were normalized for background scattering and beam transmission. Tensile measurements were obtained for samples equilibrated in liquid water and ambient air at room temperature. The wet or dry membranes were cut into a dumbbell shape (12 mm × 3 mm in the test area), and tensile measurements were performed using an Instron-5866 (Norwood, MA) instrument at a crosshead speed of 5 mm/min at room temperature (25 °C). Thermogravimetric analysis (TGA) was performed on a TGA Q50 (TA Instruments, New Castle, DE) using samples (5 mg) placed in an Al_2O_3 crucible. The samples were heated from 30 to 650 °C at a rate of 5 °C/min under flowing nitrogen (40 mL/min).

To obtain the titrated gravimetric ion exchange capacity (IEC) values, AEMs in the OH^- form were immersed in 50 mL of 0.01 M HCl standard solution for 24 h. The solutions were then titrated with a standardized NaOH (0.01 M) solution to pH = 7. The membrane was washed and immersed in deionized water for 24 h to remove any residual HCl, and then dried under vacuum conditiona at 45 °C for 24 h and weighed to determine the dry mass (in Cl^- form). The IEC of the membrane is calculated with eq 1:

$$\mathrm{IEC} = \frac{n_{i(H^+)} - n_{f(H^+)}}{m_{dry}(Cl)} \quad (1)$$

The swelling ratio was obtained by measuring the dimensions of membranes in both dry (in Br^- form) and wet (in OH^- form) states and calculated from the ratio of the change of dimension to the membrane dimension in the dry state. Water uptake (WU) was measured after drying the membrane in hydroxide form at 60 °C under vacuum conditions for 12 h. The dried membrane was immersed in water and periodically weighed on an analytical balance until a constant mass was obtained, giving the mass-based water uptake. The hydration number (λ) was calculated from eq 2:

$$\lambda = \frac{1000 \times \mathrm{WU}}{M_{H_2O} \times \mathrm{IEC}} \quad (2)$$

where M_{H_2O} is the molecular mass of water (18.015 g/mol) and IEC is the ion exchange capacity by titration.

In-plane conductivity (σ) of the membrane was obtained using eq 3:

$$\sigma = \frac{d}{R \times L_s \times W_s} \quad (3)$$

where d is the distance between the electrodes, R is the membrane resistance, and L_s and W_s are the thickness and width of the membrane, respectively. The membrane impedance was measured over the frequency range from 100 mHz to 100 kHz by two-point probe alternating current (AC) impedance spectroscopy using an impedance/gain-phase analyzer (Solartron 1260A, Solartron Analytical, Farnborough Hampshire, ONR, UK). The hydroxide conductivity measurements at temperatures ranging from 30 to 80 °C under fully

DOI: 10.1021/acs.chemmater.5b02557
Chem. Mater. 2015, 27, 6689−6698

hydrated conditions in the longitudinal direction were carried out with the cell immersed in water, which was degassed and blanketed with flowing ultrahigh-purity (UHP) argon to preserve the OH^- form of the sample.

The effective diffusion coefficient (D) of the mobile ion in AEMs was calculated from a form of the Nernst−Einstein equation:

$$D = \frac{\sigma RT}{cz^2F^2} \tag{4}$$

where σ is the measured conductivity, R is the ideal gas constant, T is temperature, c is the computed concentration of ions calculated by eq 5, z is valence charge, and F is Faraday's constant.[60]

$$c = 0.001 \times \frac{\rho \times \mathrm{IEC}}{1 + 0.01X_{\text{v-H}_2\text{O}}} \tag{5}$$

where ρ is the density of the tested polymer, which is measured by a buoyancy method, and $X_{\text{v-H}_2\text{O}}$ is the volume-based water uptake. To determine the barrier to ion transport, the calculated D was compared to the ion diffusivity in dilute solution (D_0, calculated from eq 6), the maximum diffusivity of an ion in water.[60]

$$D_0 = \frac{\mu k_B T}{q} \tag{6}$$

where μ is the dilute solution ion mobility, k_B is the Boltzmann constant, T is temperature, and q is the ion charge.[60]

Gel fraction was used to assess the extent of cross-linking in the SIPN membrane. To calculate the gel fraction, the cross-linked membrane was immersed in NMP at 80 °C for 1 day. The gel fraction was equal to the ratio of the remaining weight of the polymer after immersing in solvent to its initial weight before the immersion. The chemical stability test was conducted by immersing a piece of AEM membrane (50 ± 3 μm in thickness) in 1 M NaOH solution and was maintained at 80 °C for 30 days. Periodically during the stability test, the IEC, ionic conductivity, water uptake, maximum tensile stress, and elongation at break of AEMs were tested to evaluate the changes of the materials under strong alkaline degradation conditions.

RESULTS AND DISCUSSION

Synthesis and Characterization of SIPN AEMs. The synthesis of SIPN membranes entailed three main steps: (1) the preparation of QAPPO, (2) the synthesis of PEG−PAGE, and (3) the formation of cross-linked networks. First, the brominated PPO (BrPPO) with different degrees of bromination (DB) was reacted with trimethylamine (TMA) to produce the quaternized PPO (QAPPO) (Figure 1a). Figure 2a shows a typical ^{1}H NMR spectrum for the resultant QAPPO material; peaks were observed at chemical shifts (δ) of 4.3 and 3.1 ppm corresponding to the H atoms in the benzyl group and the quaternary ammonium group, respectively. In this work, by setting the DB of BrPPO at 30, 40, 60, and 95%, QAPPO samples with different calculated IECs ranging from 2.17 to 4.97 mmol/g (Table 1) were obtained. The experimental IECs tested by both ^{1}H NMR and titration methods (Table 1) were close to those calculated from the ideal chemical structures, indicating that the quaternization reaction can be conducted effectively under the applied conditions.

The copolymer PEG−PAGE was synthesized through anionic ring-opening polymerization of AGE with a hydroxyl-terminated PEG (M_w= 4000 g/mol) as the macroinitiator (Figure 1b). After purification, ^{1}H NMR and GPC analyses were employed to determine the composition of PEG−PAGE. By comparing the ^{1}H NMR signals from the protons in the $-CH{=}CH_2$ ($\delta\sim$ 5.0 to 6.0 ppm) of PAGE with the signals from the ether protons in PEG ($\delta\sim$ 3.3 to 3.8 ppm), the molecular weight (M_w) of the copolymer was calculated to be

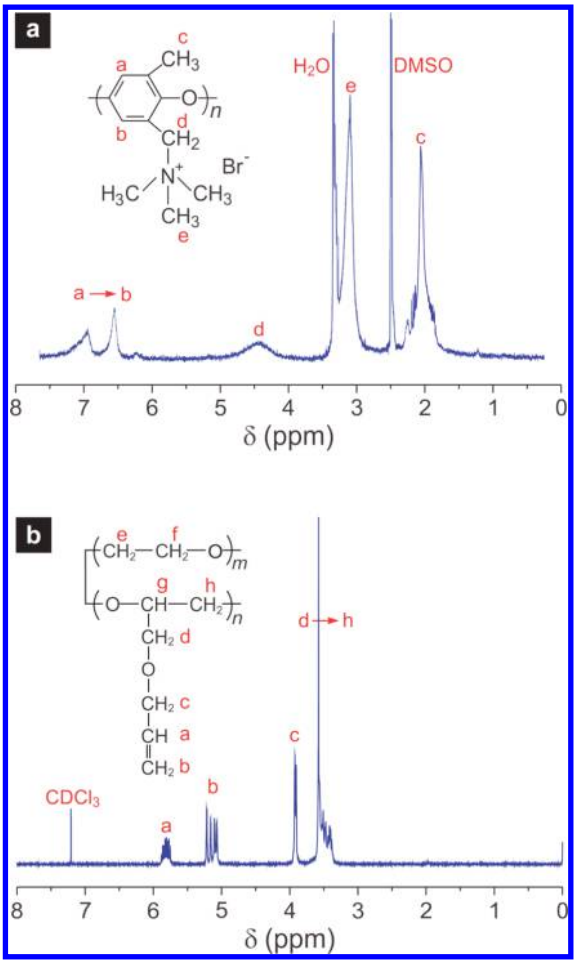

Figure 2. ^{1}H NMR of (a) QAPPO in bromine form in DMSO-d_6 and (b) PEG−PAGE in $CDCl_3$.

25.1 kg/mol, while the weight percentage of PAGE in the copolymer was approximately 84% (Figure 2b). In GPC analysis, the value of M_w of PEG−PAGE was 22.1 kg/mol, with a polydispersity (M_w/M_n) of 1.24.

QAPPO has been used extensively as an AEM in fuel cell applications, and similar to other rigid AEMs, QAPPO has shown high mechanical strength but low flexibility (Table 2). Physical blending of QAPPO with a flexible material could be a simple way to make tougher QAPPO membranes. However, when the flexible PEG−PAGE was physically mixed in solution with QAPPO and cast, these two polymers exhibited obvious macroscopic phase separation (Figure 3a). To intimately blend the PEG−PAGE and QAPPO materials, a cross-link, formed by a thiol−ene reaction between the double bonds located at the end of the side chain of PEG−PAGE and a dithiol, was introduced into the two-component system to form a homogeneous semi-interpenetrating network (Figure 3b−d). Generally, a thiol−ene coupling reaction must be triggered by a radical initiator.[59,61−64] However, in the present study, we found that the cross-linking reaction can occur effectively at elevated temperatures during membrane casting without being triggered by chemical or photoinitiation. FTIR spectroscopy (Figure 4a) was used to monitor the reaction steps for synthesizing the SIPN AEMs. Compared with pristine QAPPO, a strong ether band appeared at 1109 cm^{-1}, and the absorption bands from the pendant allyl group of the side chain at 1727 and 921 cm^{-1} in PEG−PAGE suggested the presence of flexible

DOI: 10.1021/acs.chemmater.5b02557
Chem. Mater. 2015, 27, 6689−6698

Table 1. Physical Properties of AEMs Tested at Room Temperature

sample	$W_{BrPPO}/W_{PEG-PAGE}$ (%)	IEC[a] (mmol/g)	IEC[b] (mmol/g)	IEC[c] (mmol/g)	σ_{OH^-} (mS/cm)	water uptake (%)	C_{OH^-} (mmol/cm^3)	gel fraction(%)
QAPPO-30	0	2.17	2.12	2.05	14.5	42.5	1.59	0
QAPPO-40	0	2.68	2.36	2.27	22.5	72.2	1.45	0
QAPPO-60	0	3.52	3.34	3.22	33.6	457.0	0.60	0
QAPPO-95	0	4.97	4.89					0
SIPN-60-1	1:1	1.38		1.02	13.7	51.7	0.75	96
SIPN-60-2	2:1	1.98		1.43	29.0	96.5	0.80	92
SIPN-60-3	3:1	2.32		1.74	37.4	169.4	0.70	83
SIPN-95-1	1:1	1.78		1.33	18.8	105.6	0.71	92
SIPN-95-2	2:1	2.56		1.75	35.5	213.1	0.60	89

[a]Ideal IEC calculated from polymer composition and the degree of functional group. [b]Real IEC calculated from ^{1}H NMR. [c]Real IEC tested by titration.

Table 2. Mechanical Properties of OH$^-$ Type AEMs at Dry and Wet State[a]

	tensile strength (MPa)		elongation at break (%)	
sample	dry	wet	dry	wet
QAPPO-40	51.7	21.9	18.9	37.5
QAPPO-60	22.2	7.2	14.8	13.7
SIPN-60-1	30.8	15.5	82.9	97.6
SIPN-60-2	36.4	17.4	77.0	93.4

[a]Properties measured at room temperature.

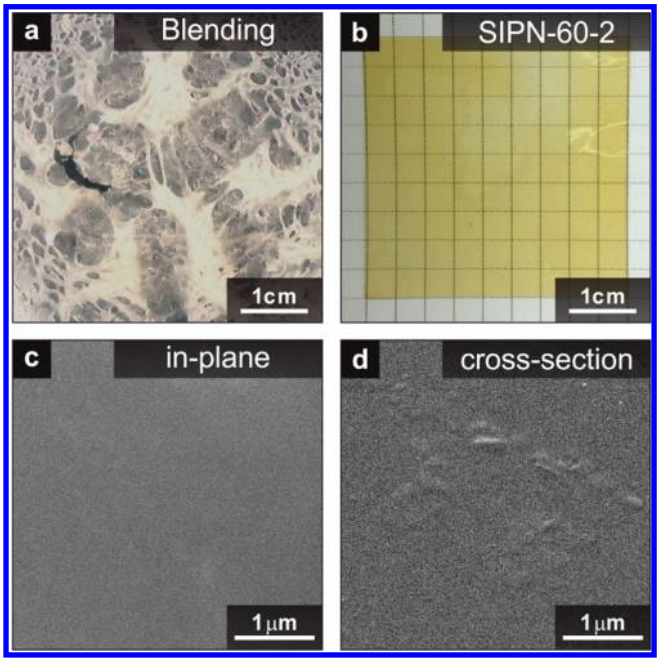

Figure 3. Compatibility of rigid QAPPO and flexible PEG−PAGE in different membranes. Photos for (a) blending of QAPPO and PEG−PAAGE and (b) SIPN-60-2 and the SEM images of (c) in-plane and (d) cross-section of SIPN-60-2.

polymer in the blend of QAPPO and PEG−PAGE (QAPPO-60 and PEG−PAGE). After the cross-linking reaction, the characteristic absorption bands from the double bonds disappeared in SIPN-60-2, which demonstrated the formation of the cross-link between the flexible polymer chains. XPS signal for S's 2p electron (the binding energies of S $2p_{1/2}$ and $2p_{3/2}$ were 164.6 and 163.5 ev respectively) in SIPN-60-2 confirmed the state of S in the membrane was thiol (R-SH) or thioether (R-S-R).[65]

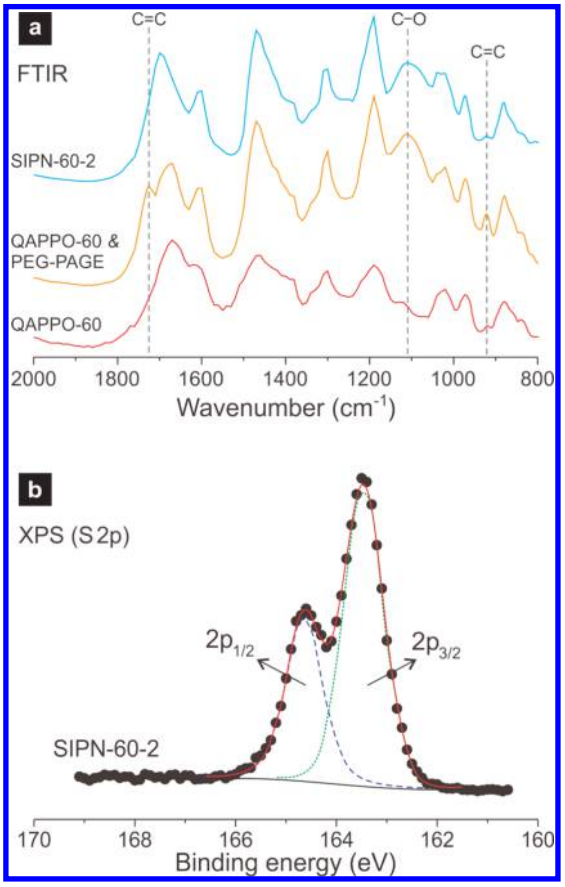

Figure 4. Evidence of the formation of cross-links in SIPN membranes. (a) FTIR of QAPPO-60, blend of QAPPO-60 and PEG−PAGE, and SIPN-60-2. (b) XPS signal for S's 2p electron in SIPN-60-2.

Mechanical Properties of SIPN AEMs. The comparison of mechanical properties between AEMs with different structures and compositions are shown in Figure 5. Upon introducing a flexible network into QAPPO, the tensile behavior of the samples could be tuned depending on the SIPN composition (Figure 5a). As conventional rigid AEMs, QAPPO-30 and QAPPO-40 showed high tensile strength above 20 MPa, but their flexibilities were low, on the order of 30−40% elongation to break (Figure 5b and c). QAPPO-60 with an IEC of 3.22 mmol/g showed low strength and flexibility. Previous work has demonstrated that the process for achieving brominated polymer with high DB would reduce the

DOI: 10.1021/acs.chemmater.5b02557
Chem. Mater. 2015, 27, 6689−6698

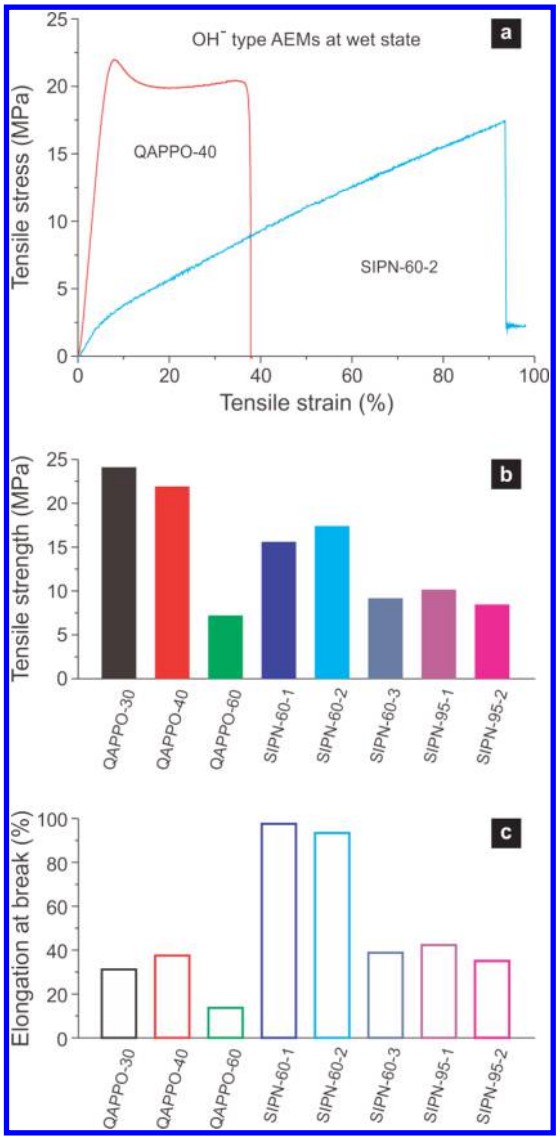

Figure 5. Mechanical properties for AEMs in OH^- form. (a) Typical stress–strain curves for QAPPO-40 and SIPN-60-2. (b) Maximum tensile stress and (c) elongation at break for different AEMs.

molecular weight (MW) of the product.[66,67] To verify the effect of DB on the MW, GPC analyses were conducted for BrPPOs with different DBs. As shown in Table S1, lower M_n and greater PDI were observed in BrPPO-60 (the precursor for QAPPO-60 synthesizing), which were responsible for the comparatively poor mechanical properties of the QAPPO-60 membrane. In addition, the large amount of ionic groups could disrupt the inter chain interactions of QAPPO-60 and may also be a reason for the low strength and flexibility of the material. In the wet state, the extremely high water uptake (Table 1) of highly functionalized samples weakened the ionic interactions between polymer chains, which resulted in poor mechanical properties in QAPPO-60 membranes. In comparison to QAPPO membranes, SIPN-60-1 and SIPN-60-2 membranes showed much higher elongation at break, especially for dry films (Table 2). The flexible network enhanced the toughness of the AEMs significantly, while their tensile strengths were maintained at relatively high levels (Table 2).

To evaluate the effect of the composition on the mechanical properties of SIPN AEMs, five samples fabricated by cross-linked PEG–PAGE and QAPPO-60 (QAPPO-60-1, QAPPO-60-2, and QAPPO-60-3) or QAPPO-95 (QAPPO-95–1 and QAPPO-95-2) were obtained. The SIPN AEMs showed superior properties to those of their QAPPO precursors (the mechanical properties of QAPPO-95 were too poor to be measured). And the SIPN-60 films based on QAPPO-60 exhibited higher strength and flexibility than those of SIPN-95 membranes based on QAPPO-95.

Elongation at break increased by raising the content of PEG–PAGE (Figure 5c), as expected. However, the increase in the PEG–PAGE fraction reduced the content of rigid QAPPO, which decreased the strength of the AEMs. Fortunately, increasing the content of PEG–PAGE in the sample caused an increase in the cross-linking degree (see gel fraction in Table 1). The increased PEG–PAGE fraction and cross-linking decreased the IEC and water uptake (Table 1), which helped to maintain good tensile strength of the SIPN membranes (Figure 5b). Among the studied SIPN AEMs, SIPN-60-1 and SIPN-60-2 showed superior qualities with tensile strengths of 15.5 and 17.4 MPa, while the elongation at break reached 97.5 and 93.4%, respectively.

Ion Conduction and Water Uptake of SIPN AEMs. The trade-off between conductivity and swelling properties is a barrier to high-performance AEM development. As depicted in Figure 6a, QAPPO-30 and -40 showed a low water uptake and swelling ratio, the swelling ratio of which was controlled at 5.8 and 15.7%, respectively, even at 80 °C. However, the low swelling ratio was accompanied by low conductivity. The OH^- conductivity of QAPPO-40 with an IEC of 2.27 mmol/g was 49.9 mS/cm at 80 °C. OH^- conductivity can be improved by

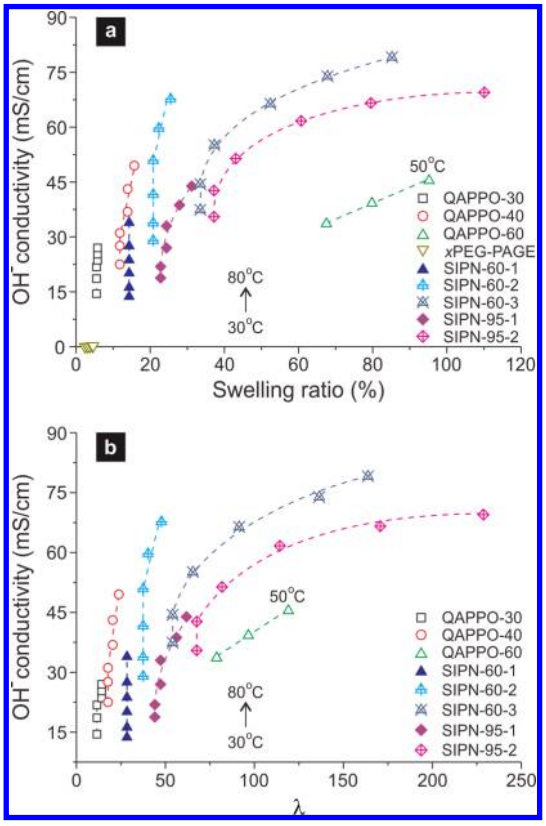

Figure 6. Comprehensive evaluation of different membranes. The OH^- conductivity as a function of (a) swelling ratio and (b) hydration number (λ), respectively.

DOI: 10.1021/acs.chemmater.5b02557
Chem. Mater. 2015, 27, 6689–6698

further increasing the IEC of QAPPO. For example, QAPPO-60 with an IEC of 3.22 mmol/g showed a conductivity of 33.6 mS/cm at room temperature, which increased to 45.4 mS/cm at 50 °C (Figure 6a). Unfortunately, enhancing ionic conductivity by increasing the IEC usually leads to a sacrifice in mechanical properties. QAPPO-60 with a high swelling ratio exhibited very poor strength and flexibility (Table 2), which is definitely not suitable for the fuel cell applications.

Compared to QAPPO, SIPN AEMs maintained a good balance between ionic conductivity and swelling ratio. Introducing the hydrophilic, cross-linked PEG−PAGE network into QAPPO with a high IEC (e.g., QAPPO-60 or QAPPO-95) partly restricted the swelling of the material and maintained a high hydration number in the SIPN membrane to ensure sufficient conductivity. As is shown in Figure 6, SIPN-60-2 ($W_{QAPPO\text{-}60}/W_{PEG-PAGE}$ = 2:1, IEC = 1.43 mmol/g) had a moderate swelling ratio (25.5% at 80 °C) and hydration number (λ = 47.8 at 80 °C), and the conductivity of the sample reached 30 and 67.7 mS/cm at 30 and 80 °C, respectively.

Reducing the content of PEG−PAGE and increasing the IEC of the QAPPOs can raise the IEC of SIPN AEMs. As a consequence, more water was absorbed in the membrane, which led to significant increases in the swelling ratio and a slight increase of conductivity. For example, at 80 °C, the swelling ratio of SIPN-60-3 ($W_{QAPPO\text{-}60}/W_{PEG-PAGE}$ = 3:1, IEC = 1.74 mmol/g) and SIPN-95-2 ($W_{QAPPO\text{-}95}/W_{PEG-PAGE}$ = 2:1, IEC = 1.75 mmol/g) were 85.2 and 110.1%, with ionic conductivities of 79.1 and 69.5 mS/cm, respectively. On the contrary, if the amount of PEG−PAGE increased, the IEC, swelling ratio, hydration number, and conductivity were all reduced. SIPN-60-1 ($W_{QAPPO\text{-}60}/W_{PEG-PAGE}$ = 1:1), with a low IEC of 1.02 mmol/g, showed a low swelling ratio of 14.3% with a conductivity of 33.9 mS/cm at 80 °C.

It is important to observe that the IECs of SIPN-60-2 (IEC 1.43 mmol/g), SIPN-60-3 (IEC 1.74 mmol/g), and SIPN-95-2 (IEC 1.75 mmol/g) were lower, but both the swelling ratios and the ionic conductivities of these samples were greater than those of QAPPO-30 (IEC 2.05 mmol/g) and −40 (IEC 2.27 mmol/g) membranes (Figure 6a). The high DB of the QAPPO as well as the strong hydrophilic nature of the PEG−PAGE network were both favorable for achieving higher hydration numbers (Figure 6b), which brought about a large swelling ratio in the SIPN membrane. Since the PEG−PAGE flexible network showed no ion conduction capability (Figure 6a), the main reason for lower IEC but higher conductivity in SIPN AEMs was attributed to the synergistic effects of the hydrophilic PEG and potential phase separation on a nanoscale in the SIPN. The first possibility for constructing highly efficient ionic channels is to induce obvious hydrophilic/hydrophobic microphase separation. However, both the SAXS data and the TEM images demonstrated that there was no pronounced ion aggregation or nanophase domains in the SIPN AEM samples, and the microphase morphology of SIPN AEM was similar to that of QAPPO film (Figure S1). Another way to obtain high conductivity in these materials is to increase the hydration number of the AEM. As shown in Figure 7, increasing the hydration number would decrease the ion concentration (c), but the normalized diffusion coefficient (D/D_0) improved significantly as the high water uptake ensured unrestricted paths for ion conduction. Specifically, SIPN-60-2, SIPN-60-3, and SIPN-95-2 with relatively low OH^- concentrations of 0.80, 0.70, and 0.60 mmol/cm^3 showed high D/D_0's of 0.49, 0.72, and 0.80, respectively, compared to the low

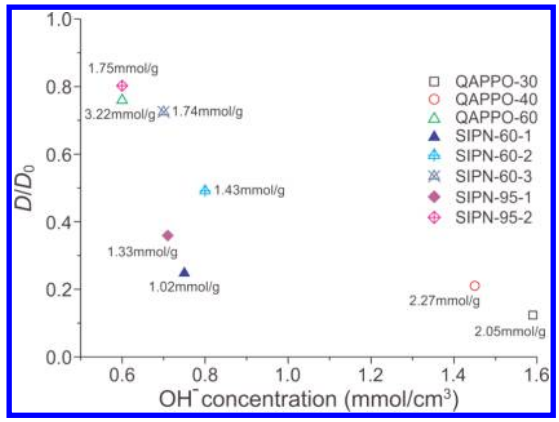

Figure 7. Ratio of the effective diffusion coefficient, D, to the diluted solution diffusivity, D_0, as a function of OH^- concentration for AEMs in OH^- form at room temperature.

mobilities of QAPPO-30 (D/D_0 = 0.12) and -40 (D/D_0 = 0.21).

Alkaline Stability. Conductivity of AEMs can be increased by a number of methods, but long-term chemical stability is currently preventing the demonstration of long-lived AEMFCs and other alkaline membrane electrochemical devices. It is hypothesized that the overall stability of AEMs is determined by the degradation of the cation and polymer backbone under alkaline conditions. Groups with a strong electrophilic nature (e.g., quaternary ammonium) are very likely to be attacked by OH^-, especially at elevated temperatures.[20] To evaluate the alkaline stability of SIPN AEMs, SIPN-60-2, SIPN-60-3, QAPPO-30, and QAPPO-40 were immersed in 1 M NaOH solution at 80 °C for 1 month with replacement of the 1 M NaOH every 3 days during the testing period. Evaluation of OH^- stability at 80 °C over long times is important because many studies have shown stability of a variety of AEMs at 60 °C, but the degradation environment is much more challenging at 80 °C where few samples have demonstrated and verified long-term stability. As shown in Figure 8, although the chemical structure of the cation and the polymer backbone of the polyelectrolyte in SIPN AEMs were the same as those of the QAPPO, SIPN AEMs showed much higher cation stability under alkaline conditions. After 30 days of immersion, the IECs of QAPPO-30 and -40 decreased by 41.5% and 56.8%, and the OH^- conductivities decreased by 42.9% and 61.2%, respectively. In contrast, the IEC values of SIPN-60-2 (IEC = 1.43 mmol/g) and −3 (IEC = 1.74 mmol/g) films decreased to 1.09 mmol/g and 1.17 mmol/g, and the OH^- conductivity values were maintained at 52.4 mS/cm and 55.7 mS/cm at 80 °C, about 20−30% lower than the values measured for the sample before the stability test. Lower initial IECs could be responsible for the higher stability of the AEMs. Furthermore, with similar IECs, the SIPN-60-3 (IEC = 1.74 mmol/g, DB = 60%) membrane also exhibited higher stability than that of QAPPO-30 (IEC = 2.05 mmol/g, DB = 30%). The degradation of anion exchange membrane samples is likely dependent on the water uptake and the degree of bromination of the quaternary ammonium polymer backbone. These factors, along with the IEC and molecular weight of the polymer, must be considered as work progresses on understanding the molecular details that contribute to membrane degradation. The additional flexible network, which guaranteed high dimensional stability for the SIPN membranes, may change the environment around the

DOI: 10.1021/acs.chemmater.5b02557
Chem. Mater. 2015, 27, 6689−6698

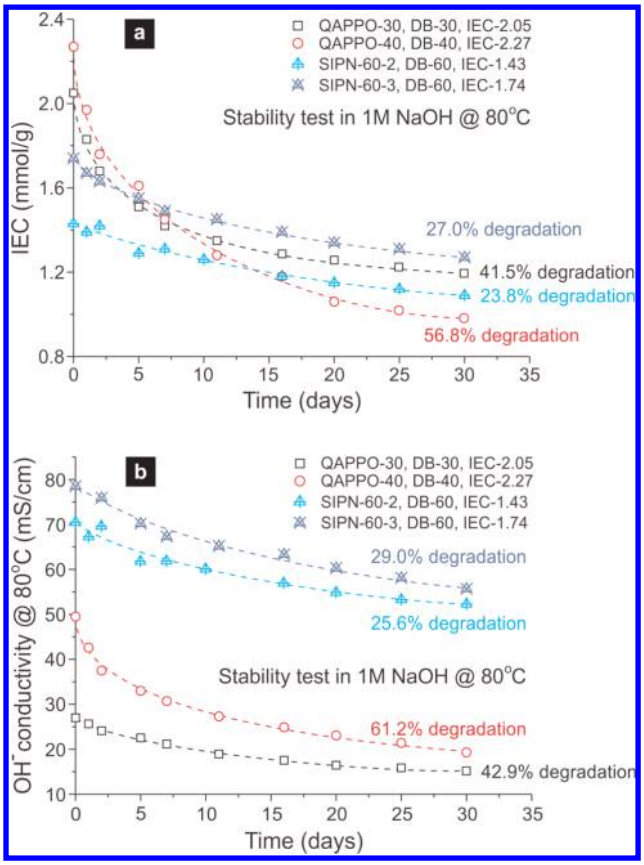

Figure 8. Chemical stability of the quaternary ammonium cation of QAPPO-30 (DB = 30, IEC = 2.05 mmol/g), QAPPO-40 (DB = 40, IEC = 2.27 mmol/g), SIPN-60-2 (DB = 60, IEC = 1.43 mmol/g), and SIPN-60-3 (DB = 60, IEC = 1.74 mmol/g) in 1 M NaOH solution at 80 °C. (a) OH^- conductivity measured at 80 °C and (b) IEC as a function of duration time.

QAPPO chain and potentially protect it from the severe nucleophilic attack by hydroxide ions.

Additionally, having a hydroxide resistant cross-linked network hinders mechanical degradation of the sample. SIPN-60-2 exhibited superior mechanical stabilities to pure QAPPO samples. The immersion of QAPPO-40 film in a hot alkaline solution weakened the interaction between the polymer chains, resulting in a large swelling of this AEM. The water uptake of QAPPO-40 increased to 187.5 and 270.0% after 15 and 30 days of degradation testing, respectively, compared to an initial water uptake of 72.2%. After 15 days of degradation, the strength and flexibility of QAPPO-40 decreased by almost 50%. After 18 days of aging, the film began to break into small pieces, and its tensile behavior could not be determined. Relative to QAPPO-40, good strength retention and flexibility were observed in the SIPN-60-2 membrane. The mechanical strength was maintained at 14.6 and 12.5 MPa, and the elongation of break maintained 78 and 69% of the original values after 15 and 30 days of stability testing, respectively. The highly alkaline-tolerant PEG−PAGE flexible network restrained further swelling of the SIPN AEM, which only slightly increased in water uptake after the 30-day aging period (Table 3). In addition to testing the mechanical stabilities in 1 M NaOH solution, we evaluated the changes of the mechanical properties of the samples in 3 M NaOH at 80 °C (Figure S2). Increasing the concentration of alkaline solution from 1 to 3 M showed no obvious influence on the mechanical properties of the AEM samples; therefore increasing the base concentration did not lead to more severe degradation of the materials. Since all the stability tests were conducted in 250 mL of solution, there was a large excess of OH^- during the test. Due to this large excess, the higher concentration (3 M) may not cause a significant change of the environment surrounding the films, and thus similar degradation rates were observed in these two solutions.

CONCLUSIONS

In summary, we have designed and synthesized AEMs based on a rigid-flexible semi-interpenetrating network (SIPN) for fuel cell applications. Quaternized PPO (QAPPO) with relatively high IEC was chosen as a rigid and conductive functional phase, while a hydrophilic and highly alkali-resistant PEG−PAGE thermally cross-linked by dithiol was employed as the flexible network. The addition of the flexible network sharply increased the flexibility of the QAPPO-based AEM; the elongation at break of wet SIPN-60-2 film reached 93.4% with a high mechanical strength of 17.4 MPa. High conductivity and water uptake were observed in SIPN AEMs since such membranes exhibited high hydration numbers even at low IECs. High hydration numbers increase the membrane swelling and decrease the ion concentration but effectively enhanced the ion mobility in these AEMs. For example, SIPN-60-2 with the IEC of 1.43 mmol/g showed an ionic conductivity of 67.7 mS/cm and a swelling ratio of 25.5% at 80 °C, which were higher than that of the properties of the QAPPO-40 membrane with an IEC of 2.27 mmol/g (the ionic conductivity is 49.9 mS/cm and the swelling ratio is 15.7% at 80 °C).

In addition to improved physical properties, SIPN AEMs exhibited excellent alkaline stability. The quaternary ammonium cation in SIPN-60-2 showed much higher chemical stability than the same group in QAPPO-40. After testing the AEMs in 1 M NaOH solution at 80 °C for 30 days, the decreases in IEC and conductivity of SIPN-60-2 were less than half of those for QAPPO-40. Meanwhile, SIPN-60-2 showed good dimensional and mechanical stabilities in hot alkaline solution and changed only slightly after the long-term aging test.

Table 3. Mechanical Properties and Water Uptakes of AEMs before and after Stability Test in Hot Alkaline Solution[a]

	tensile strength (MPa)		elongation at break (%)		water uptake (%)	
time (days)[b]	SIPN-60-2	QAPPO-40	SIPN-60-2	QAPPO-40	SIPN-60-2	QAPPO-40
0	17.4	21.9	93.4	37.5	124.6	72.2
15	14.6 (↓16.1%)	11.2 (↓48.9%)	77.7 (↓16.8%)	19.6 (↓47.7%)	129.4 (↑3.9%)	187.5 (↑159.7%)
30	12.5 (↓28.2%)		69.1 (↓26.0%)		138.1 (↑10.8%)	270.0 (↑274.0%)

[a]Properties measured at room temperature. [b]The time for AEMs immersed in 1 M NaOH solution at 80 °C.

DOI: 10.1021/acs.chemmater.5b02557
Chem. Mater. 2015, 27, 6689−6698

■ ASSOCIATED CONTENT

Supporting Information

The Supporting Information is available free of charge on the ACS Publications website at DOI: 10.1021/acs.chemmater.5b02557.

SAXS and TEM images of QAPPO-60 and QAPPO-60-2, mechanical properties for SIPN-60-2 and QAPPO-40 membrane before and after stability test in 1 and 3 M NaOH solutions at 80 °C for 15 days, FTIR spectra for SIPN-60-2 film before and after stability test in 1 M NaOH solution at 80 °C for 30 days, XPS spectra for SIPN-60-2 film before and after stability test in 1 M NaOH solution at 80 °C for 30 days, and TGA curves for QAPPO-60, *x*PEG−PAGE, and SIPN-60-2 samples (PDF)

■ AUTHOR INFORMATION

Corresponding Author

*E-mail: mah49@psu.edu.

Notes

The authors declare no competing financial interest.

■ ACKNOWLEDGMENTS

The authors would like to acknowledge our industrial sponsors. This work was funded in part by the Advanced Research Projects Agency—Energy (ARPA-E), U.S. Department of Energy, under award number DE-AR0000121, and the United States−Israel Binational Science Foundation (BSF) through Energy Project No. 2011521. Infrastructure support was also provided by The Pennsylvania State University Materials Research Institute and the Penn State Institutes of Energy & the Environment.

■ REFERENCES

(1) Jacobson, M. Z.; Colella, W. G.; Golden, D. M. Cleaning the air and improving health with hydrogen fuel-cell vehicles. *Science* **2005**, *308*, 1901−1905.

(2) Hickner, M. A.; Ghassemi, H.; Kim, Y. S.; Einsla, B. R.; McGrath, J. E. Alternative polymer systems for proton exchange membranes (PEMs). *Chem. Rev.* **2004**, *104*, 4587−4612.

(3) Steele, B. C. H.; Heinzel, A. Materials for fuel-cell technologies. *Nature* **2001**, *414*, 345−352.

(4) Kreuer, K.-D. Proton conductivity: Materials and applications. *Chem. Mater.* **1996**, *8*, 610−641.

(5) Choi, P.; Jalani, N. H.; Datta, R. Thermodynamics and proton transport in Nafion II. Proton diffusion mechanisms and conductivity. *J. Electrochem. Soc.* **2005**, *152*, E123−E130.

(6) Liu, D.; Kyriakides, S.; Case, S. W.; Lesko, J. J.; Li, Y.; McGrath, J. E. Tensile behavior of Nafion and sulfonated poly(arylene ether sulfone) copolymer membranes and its morphological correlations. *J. Polym. Sci., Part B: Polym. Phys.* **2006**, *44*, 1453−1465.

(7) Debe, M. K. Electrocatalyst approaches and challenges for automotive fuel cells. *Nature* **2012**, *486*, 43−51.

(8) Eisenberg, A.; Yeager, H. L. *Perfluorinated Ionomer Membranes*; ACS Symposium Series 180; American Chemical Society: Washington, DC, 1982.

(9) Tant, M. R.; Kauritz, K. A.; Wilkes, G. L. *Ionomers*; Chapman & Hall: UK, 1997.

(10) Wu, G.; More, K. L.; Johnston, C. M.; Zelenay, P. High-performance electrocatalysts for oxygen reduction derived from polyaniline, iron, and cobalt. *Science* **2011**, *322*, 443−447.

(11) Bashyam, R.; Zelenay, P. A class of non-precious metal composite catalysts for fuel cells. *Nature* **2006**, *443*, 63−66.

(12) Jo, T. S.; Ozawa, C. H.; Eagar, B. R.; Brownell, L. V.; Han, D.; Bae, C. Synthesis of sulfonated aromatic poly(ether amide)s and their application to proton exchange membrane fuel cells. *J. Polym. Sci., Part A: Polym. Chem.* **2009**, *47*, 485−496.

(13) Miyatake, K.; Chikashige, Y.; Higuchi, E.; Watanabe, M. Tuned polymer electrolyte membranes based on aromatic polyethers for fuel cell applications. *J. Am. Chem. Soc.* **2007**, *129*, 3879−3887.

(14) Asano, N.; Aoki, M.; Suzuki, S.; Miyatake, K.; Uchida, H.; Watanabe, M. Aliphatic/aromatic polyimide ionomers as a proton conductive membrane for fuel cell applications. *J. Am. Chem. Soc.* **2006**, *128*, 1762−1769.

(15) Hu, Q.; Li, G.; Pan, J.; Tan, L.; Lu, J.; Zhuang, L. Alkaline polymer electrolyte fuel cell with Ni-based anode and Co-based cathode. *Int. J. Hydrogen Energy* **2013**, *38*, 16264−16268.

(16) Pan, J.; Chen, C.; Zhuang, L.; Lu, J. Designing advanced alkaline polymer electrolytes for fuel cell applications. *Acc. Chem. Res.* **2012**, *45*, 473−481.

(17) Lu, S.; Pan, J.; Huang, A.; Zhuang, L.; Lu, J. Alkaline polymer electrolyte fuel cells completely free from noble metal catalysts. *Proc. Natl. Acad. Sci. U. S. A.* **2008**, *105*, 20611−20614.

(18) Asazawa, K.; Yamada, K.; Tanaka, H.; Oka, A.; Taniguchi, M.; Kobayashi, T. A Platinum-free zero-carbon-emission easy fuelling direct hydrazine fuel cell for vehicles. *Angew. Chem., Int. Ed.* **2007**, *46*, 8024−8027.

(19) Varcoe, J. R.; Slade, R. C. T. Prospects for alkaline anion-exchange membranes in low temperature fuel cells. *Fuel Cells* **2005**, *5*, 187−200.

(20) Varcoe, J. R.; Atanassov, P.; Dekel, D. R.; Herring, A. M.; Hickner, M. A.; Kohl, P. A.; Kucernak, A. R.; Mustain, W. E.; Nijmeijer, K.; Scott, K.; Xu, T.; Zhuang, L. Anion-exchange membranes in electrochemical energy systems. *Energy Environ. Sci.* **2014**, *7*, 3135−3191.

(21) Wang, Y.-J.; Qiao, J.; Baker, R.; Zhang, J. Alkaline polymer electrolyte membranes for fuel cell applications. *Chem. Soc. Rev.* **2013**, *42*, 5768−5787.

(22) Hickner, M. A.; Herring, A. M.; Coughlin, E. B. J. Anion exchange membranes: Current status and moving forward. *J. Polym. Sci., Part B: Polym. Phys.* **2013**, *51*, 1727−1735.

(23) Pan, J.; Li, Y.; Han, J.; Li, G.; Tan, L.; Chen, C.; Lu, J.; Zhuang, L. A strategy for disentangling the conductivity−stability dilemma in alkaline polymer electrolytes. *Energy Environ. Sci.* **2013**, *6*, 2912−2915.

(24) Pan, J.; Lu, S.; Li, Y.; Huang, A.; Zhuang, L.; Lu, J. High-performance alkaline polymer electrolyte for fuel cell applications. *Adv. Funct. Mater.* **2010**, *20*, 312−319.

(25) Gu, S.; Cai, R.; Luo, T.; Chen, Z.; Sun, M.; Liu, Y.; He, G.; Yan, Y. A soluble and highly conductive ionomer for high-performance hydroxide exchange membrane fuel cells. *Angew. Chem., Int. Ed.* **2009**, *48*, 6499−6502.

(26) Liu, L.; Li, Q.; Dai, J.; Wang, H.; Jin, B.; Bai, R. A facile strategy for the synthesis of guanidinium-functionalized polymer as alkaline anion exchange membrane with improved alkaline stability. *J. Membr. Sci.* **2014**, *453*, 52−60.

(27) Li, N.; Leng, Y.; Hickner, M. A.; Wang, C.-Y. Highly stable, anion conductive, comb-shaped copolymers for alkaline fuel cells. *J. Am. Chem. Soc.* **2013**, *135*, 10124−10133.

(28) Gu, S.; Skovgard, J.; Yan, Y. Engineering the Van der Waals interaction in cross-linking-free hydroxide exchange membranes for low swelling and high conductivity. *ChemSusChem* **2012**, *5*, 843−848.

(29) Wu, Y.; Wu, C.; Varcoe, J. R.; Poynton, S. D.; Xu, T.; Fu, Y. Novel silica/poly(2,6-dimethyl-1,4-phenylene oxide) hybrid anion-exchange membranes for alkaline fuel cells: Effect of silica content and the single cell performance. *J. Power Sources* **2010**, *195*, 3069−3076.

(30) Vandiver, M. A.; Caire, B. R.; Poskin, Z.; Li, Y.; Seifert, S.; Knauss, D. M.; Herring, A. M.; Liberatore, M. W. Durability and performance of polystyrene-b-poly(vinylbenzyl trimethylammonium) diblock copolymer and equivalent blend anion exchange membranes. *J. Appl. Polym. Sci.* **2015**, *132*, 41596.

(31) Zeng, Q. H.; Liu, Q. L.; Broadwell, I.; Zhu, A. M.; Xiong, Y.; Tu, X. P. Anion exchange membranes based on quaternized polystyrene-

DOI: 10.1021/acs.chemmater.5b02557
Chem. Mater. 2015, 27, 6689−6698

block-poly(ethylene-ran-butylene)-block- polystyrene for direct methanol alkaline fuel cells. *J. Membr. Sci.* **2010**, *349*, 237−243.
(32) Varcoe, J. R.; Slade, R. C. T.; Yee, E. L. H.; Poynton, S. D.; Driscoll, D. J.; Apperley, D. C. Poly(ethylene-co-tetrafluoroethylene)-derived radiation-Grafted anion-exchange membrane with properties specifically tailored for application in metal-cation-free alkaline polymer electrolyte fuel cells. *Chem. Mater.* **2007**, *19*, 2686−2693.
(33) Han, J.; Peng, H.; Pan, J.; Wei, L.; Li, G.; Chen, C.; Xiao, L.; Lu, J.; Zhuang, L. Highly stable alkaline polymer electrolyte based on a poly(ether ether ketone) backbone. *ACS Appl. Mater. Interfaces* **2013**, *5*, 13405−13411.
(34) Jasti, A.; Prakash, S.; Shahi, V. K. Stable and hydroxide ion conductive membranes for fuel cell applications: Chloromethyaltion and amination of poly(ether ether ketone). *J. Membr. Sci.* **2013**, *428*, 470−479.
(35) Wang, J.; Wang, J.; Zhang, S. Synthesis and characterization of cross-linked poly(arylene ether ketone) containing pendant quaternary ammonium groups for anion-exchange membranes. *J. Membr. Sci.* **2012**, *415*−*416*, 205−212.
(36) Hibbs, M. R.; Fujimoto, C. H.; Cornelius, C. J. Synthesis and characterization of poly(phenylene)-based anion exchange membranes for alkaline fuel cells. *Macromolecules* **2009**, *42*, 8316−8321.
(37) Yan, J.; Hickner, M. A. Anion exchange membranes by bromination of benzylmethyl-containing poly(sulfone)s. *Macromolecules* **2010**, *43*, 2349−2356.
(38) Hibbs, M. R.; Hickner, M. A.; Alam, T. M.; McIntyre, S. K.; Fujimoto, C. H.; Cornelius, C. J. Transport properties of hydroxide and proton conducting membranes. *Chem. Mater.* **2008**, *20*, 2566−2573.
(39) Hugar, K. M.; Kostalik, H. A., IV; Coates, G. W. Imidazolium cations with exceptional alkaline stability: A systematic study of structure−stability relationships. *J. Am. Chem. Soc.* **2015**, *137*, 8730−8737.
(40) Lin, B.; Dong, H.; Li, Y.; Si, Z.; Gu, F.; Yan, F. Alkaline stable C2-substituted imidazolium-based anion-exchange membranes. *Chem. Mater.* **2013**, *25*, 1858−1867.
(41) Aitken, B. S.; Buitrago, C. F.; Heffley, J. D.; Lee, M.; Gibson, H. W.; Winey, K. I.; Wagener, K. B. Precision ionomers: Synthesis and thermal/mechanical characterization. *Macromolecules* **2012**, *45*, 681−687.
(42) Kim, D. S.; Fujimoto, C. H.; Hibbs, M. R.; Labouriau, A.; Choe, Y.-K.; Kim, T. S. Resonance stabilized perfluorinated ionomers for alkaline membrane fuel cells. *Macromolecules* **2013**, *46*, 7826−7833.
(43) Kim, D. S.; Labouriau, A.; Guiver, M. D.; Kim, Y. S. Guanidinium-functionalized anion exchange polymer electrolytes via activated fluorophenyl-amine reaction. *Chem. Mater.* **2011**, *23*, 3795−3797.
(44) Robertson, N. J.; Kostalik, H. A., IV; Clark, T. J.; Mutolo, P. F.; Abrunã, H. D.; Coates, G. W. Tunable high performance cross-linked alkaline anion exchange membranes for fuel cell applications. *J. Am. Chem. Soc.* **2010**, *132*, 3400−3404.
(45) Pan, J.; Li, Y.; Zhuang, L.; Lu, J. Self-crosslinked alkaline polymer electrolyte exceptionally stable at 90 °C. *Chem. Commun.* **2010**, *46*, 8597−8599.
(46) Pan, J.; Chen, C.; Li, Y.; Wang, L.; Tan, L.; Li, G.; Tang, X.; Xiao, L.; Lu, J.; Zhuang, L. Constructing ionic highway in alkaline polymer electrolytes. *Energy Environ. Sci.* **2014**, *7*, 354−360.
(47) Tanaka, M.; Fukasawa, K.; Nishino, E.; Yamaguchi, S.; Yamada, K.; Tanaka, H.; Bae, B.; Miyatake, K.; Watanabe, M. Anion conductive block poly(arylene ether)s: Synthesis, properties, and application in alkaline fuel cells. *J. Am. Chem. Soc.* **2011**, *133*, 10646−10654.
(48) He, S. S.; Strickler, A. L.; Frank, C. W. A semi-interpenetrating network approach for dimensionally stabilizing highly-charged anion exchange membranes for alkaline fuel cells. *ChemSusChem* **2015**, *8*, 1472−1483.
(49) Song, F.; Fu, Y.; Gao, Y.; Li, J.; Qiao, J.; Zhou, X.-D.; Liu, Y. Novel alkaline anion-exchange membranes based on chitosan/ethenylmethylimidazoliumchloride polymer with ethenylpyrrolidone composites for low temperature polymer electrolyte fuel cells. *Electrochim. Acta* **2015**, *177*, 137−144.
(50) Park, A. M.; Turley, F. E.; Wycisk, R. J.; Pintauro, P. N. Electrospun and cross-linked nanofiber composite anion exchange membranes. *Macromolecules* **2014**, *47*, 227−235.
(51) Li, X.; Yu, Y.; Liu, Q.; Meng, Y. Synthesis and properties of anion conductive ionomers containing tetraphenyl methane moieties. *ACS Appl. Mater. Interfaces* **2012**, *4*, 3627−3635.
(52) Lin, B.; Qiu, L.; Qiu, B.; Peng, Y.; Yan, F. A soluble and conductive polyfluorene ionomer with pendant imidazolium groups for alkaline fuel cell applications. *Macromolecules* **2011**, *44*, 9642−9649.
(53) Lin, B.; Qiu, L.; Lu, J.; Yan, F. Cross-linked alkaline ionic liquid-based polymer electrolytes for alkaline fuel cell applications. *Chem. Mater.* **2010**, *22*, 6718−6725.
(54) Li, G.; Pan, J.; Han, J.; Chen, C.; Lu, J.; Zhuang, L. Ultrathin composite membrane of alkaline polymer electrolyte for fuel cell applications. *J. Mater. Chem. A* **2013**, *1*, 12497−12502.
(55) Zhao, Y.; Yu, H.; Yang, D.; Li, J.; Shao, Z.; Yi, B. High-performance alkaline fuel cells using crosslinked composite anion exchange membrane. *J. Power Sources* **2013**, *221*, 247−251.
(56) Arges, C. G.; Ramani, V. Two-dimensional NMR spectroscopy reveals cation-triggered backbone degradation in polysulfone-based anion exchange membranes. *Proc. Natl. Acad. Sci. U. S. A.* **2013**, *110*, 2490−2495.
(57) Nuñez, S. A.; Hickner, M. A. Quantitative 1H NMR analysis of chemical stabilities in anion-exchange membranes. *ACS Macro Lett.* **2013**, *2*, 49−52.
(58) Li, N.; Yan, T.; Li, Z.; Thurn-Albrecht, T.; Binder, W. H. Comb-shaped polymers to enhance hydroxide transport in anion exchange membranes. *Energy Environ. Sci.* **2012**, *5*, 7888−7892.
(59) Persson, J. C.; Jannasch, P. Block copolymers containing intrinsically proton-conducting blocks tethered with benzimidazole units. *Chem. Mater.* **2006**, *18*, 3096−3102.
(60) Disabb-Miller, M. L.; Zha, Y.; DeCarlo, A. J.; Pawar, M.; Tew, G. N.; Hickner, M. A. Water uptake and ion mobility in cross-linked bis(terpyridine) ruthenium-based anion exchange membranes. *Macromolecules* **2013**, *46*, 9279−9287.
(61) Mangold, C.; Dingels, C.; Obermeier, B.; Frey, H.; Wurm, F. PEG-based multifunctional polyethers with highly reactive vinyl-ether side chains for click-type functionalization. *Macromolecules* **2011**, *44*, 6326−6334.
(62) Obermeier, B.; Frey, H. Poly (ethylene glycol-co-allyl glycidyl ether) s: A PEG-based modular synthetic platform for multiple bioconjugation. *Bioconjugate Chem.* **2011**, *22*, 436−444.
(63) Stoica, D.; Alloin, F.; Marais, S.; Langevin, D.; Chappey, C.; Judeinstein, P. Polyepichlorhydrin membranes for alkaline fuel cells: sorption and conduction properties. *J. Phys. Chem. B* **2008**, *112*, 12338−12346.
(64) Persson, J. C.; Jannasch, P. Intrinsically proton-conducting comb-like copolymers with benzimidazole tethered to the side chains. *Solid State Ionics* **2006**, *177*, 653−658.
(65) Briggs, D. In *Surface Analysis of Polymer by XPS and Static SIMS*; Cambridge University Press: Cambridge, UK, 1998; chapter 3, p 73.
(66) Chen, D.; Hickner, M. A. Ion Clustering in quaternary ammonium functionalized benzylmethyl containing poly(arylene ether ketone)s. *Macromolecules* **2013**, *46*, 9270−9278.
(67) Yan, J.; Hickner, M. A. Anion exchange membranes by bromination of benzylmethyl-containing. *Macromolecules* **2010**, *43*, 2349−2356.

DOI: 10.1021/acs.chemmater.5b02557
Chem. Mater. 2015, 27, 6689−6698